First-principles investigation of bilayer graphene with intercalated C, N or O atoms

2010 J. Phys.: Condens. Matter 22 245502

(http://iopscience.iop.org/0953-8984/22/24/245502)

J. Phys.: Condens. Matter **22** (2010) 245502 (7pp) doi:10.1088/0953-8984/22/24/245502

First-principles investigation of bilayer graphene with intercalated C, N or O atoms

S J Gong[1,3], W Sheng[2], Z Q Yang[2] and J H Chu[1,3]

[1] National Laboratory for Infrared Physics, Shanghai Institute of Technical Physics, Chinese Academy of Sciences, Shanghai 200083, People's Republic of China
[2] National Laboratory for Surface Physics, Fudan University, Shanghai 200433, People's Republic of China
[3] Key Laboratory of Polar Materials and Devices, Ministry of Education, East China Normal University, Shanghai 200241, People's Republic of China

E-mail: sjgsitp@hotmail.com

Received 31 March 2010, in final form 30 April 2010
Published 26 May 2010
Online at stacks.iop.org/JPhysCM/22/245502

Abstract
We apply first-principles calculations to investigate the structural, electronic and magnetic properties of the bilayer graphene, into which C, N or O atoms are intercalated. The inserted atoms initially set at the middle of the bilayer interval will finally be adsorbed to one graphene layer, resulting in the difference of electrostatic potential between the two graphene layers and then an opening of the energy gap filled with impurity states. Extended or quasilocalized states around the Fermi level introduced by the intercalated atoms induce the itinerant Stoner magnetism in C- and N-intercalated systems. The magnetic moment in the N-intercalated system is mainly contributed by the N atom, while in the C-intercalated system, besides the foreign intercalated C atom, host carbon atoms of the bilayer graphene also become magnetic, with the magnetization distribution showing threefold symmetry. Also, charge transfer from bilayer graphene to the intercalated N or O atoms results in the Fermi level shifting downward to the valence band and then the metallic behavior of the system.

(Some figures in this article are in colour only in the electronic version)

1. Introduction

Ultrathin graphite films, typically graphene [1] and its bilayer [2], remain the focus of active research motivated by their novel physical properties and promising potential for applications [3–5]. Experimental researchers have enabled the preparation and study of systems with a single layer or a limited number of layers of graphene sheets [6]. Monolayer graphene (MLG) and bilayer graphene (BLG) have many similar properties, for example, they both have zero gap, and π orbitals orthogonal to the graphene planes are responsible for their electronic properties. However, MLG and BLG also show a critical difference. MLG has a linear energy dispersion relation and carriers in it can be described as massless Dirac fermions, while BLG, in which two monolayer graphene sheets combine in the usual A–B Bernal stacking, shows parabolically dispersion of both valence and conduction bands that are split from each other by the interlayer interaction [7], resulting in non-zero mass carriers.

The bilayer graphene draws special attention mainly by the tunability of its bandgap [8–16], which can be easily opened by the difference of the electrostatic potential between the two layers introduced either by chemical doping or by applying gate voltage. Angle-resolved photoemission (ARPES) measurements have confirmed such a gap in potassium-doped bilayer graphene epitaxially grown on SiC [13]. Infrared spectroscopy measurements have also detected a similar gap in the electrostatically gated bilayer graphene [9–11]. This bandgap leads to high resistance of graphene channels in the OFF state, which may be applied in future nanoelectronics. Very recently, strong suppression of electrical noise in bilayer graphene devices has been reported [17], which provides exciting opportunities for BLG in low-noise applications. All in all, BLG with its peculiar

properties occupies an irreplaceable position in graphene-related fields and attracts more and more research interest.

In the present paper, the doping effect in bilayer graphene is investigated. Different from the previous reports, in which doped atoms are adsorbed on the outside of the bilayer graphene [13], in the present investigation, foreign atoms are assumed to be intercalated between the two graphene layers of BLG. The results for systems with intercalated atoms C, N or O are presented, including their ground states, magnetic behaviors and electronic structures. It is found that the doped atom, although initially set at the middle position between the two layers of BLG, is absorbed on one graphene layer, which results in the difference of electrostatic potential between the two graphene layers and then an opening of the energy gap filled with impurity states. C- and N-intercalated systems show itinerant Stoner magnetism with extended or quasilocalized states around the Fermi level. In the N-intercalated system, the magnetic moment is mainly contributed by the N atom, while in the C-intercalated system, both the foreign intercalated C atom and the host carbon atoms of the graphene layer become magnetic, with the magnetization distribution of threefold symmetry. Also, N and O atoms can easily gain electrons from carbon atoms of bilayer graphene, which leads to the Fermi level shifting downward to the valence band and then the metallic behavior of the bilayer graphene.

2. Models and analysis

First-principles calculations and corresponding theoretical analysis were carried out to explore the electronic and magnetic properties of bilayer graphene, into which C, N or O atoms are intercalated. The calculations were performed by using the projector augmented wave (PAW) formalism of density functional theory (DFT) as implemented in the Vienna *ab initio* simulation package (VASP) [18]. Because the generalized gradient approximation (GGA) [19] gives essentially no bonding between two layers in BLG and leads to too a large value of bilayer spacing [12], the calculations within the localized density approximation (LDA) were performed. It is found that LDA gives rise to an interlayer spacing of 3.34 Å, in good agreement with the experiment value. Some previous investigations used LDA to optimize the structure with a reasonable bilayer spacing and then GGA to calculate the electronic structure [8]. To keep consistent, we used LDA in all the present calculations. The model system consists of a 4×4 supercell with one single foreign atom intercalated between the two coupled graphene layers. The supercell parameters were set as $a = b = 9.84$ Å (a and b indicate the crystal lattice constants in the xy plane). A cutoff energy of 400 eV for plane-wave expansion of the PAW was used and the Brillouin zone was sampled through a $11 \times 11 \times 1$ Γ centered k-point grid, which was proved enough to yield reliable convergence of the Hellmann–Feynman forces (less than 0.01 eV Å^{-1}) by test calculations with higher cutoff energy and more dense sampling of the Brillouin zone. For geometry optimization, all internal coordinates were relaxed until the Hellmann–Feynman forces were less than 0.01 eV Å^{-1}. The vacuum thickness along the z axis was 16 Å to avoid the interaction between adjacent supercells [2].

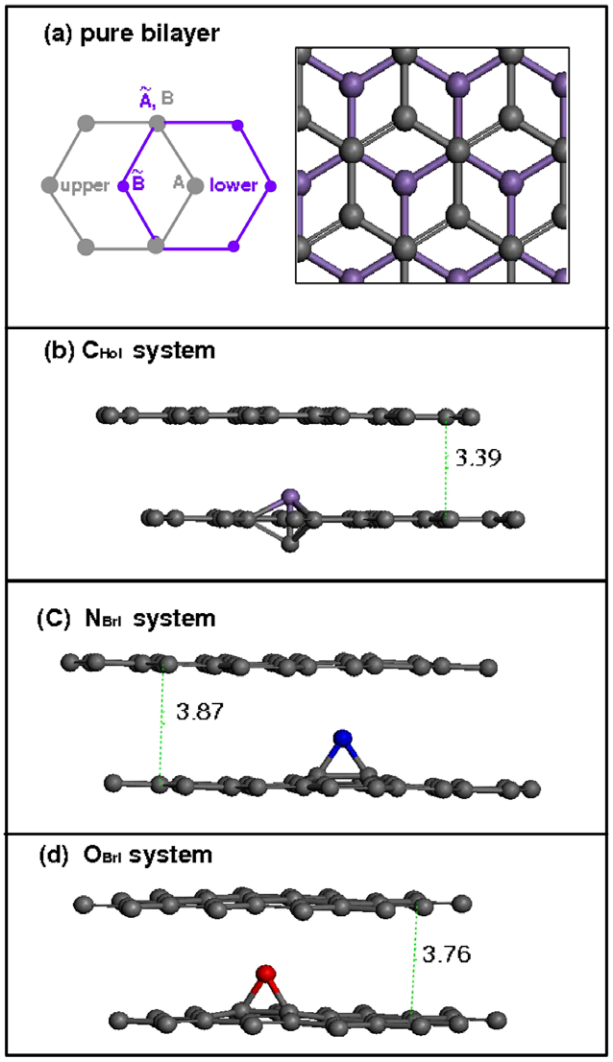

Figure 1. (a) Bernal stacking structure for bilayer graphene. (b) Ground state of C-intercalated system (C_{Hol}), where the atom in violet (gray) is the foreign C atom. (c) Ground state of N-intercalated system (N_{Bri}), where the atom in blue (dark) is the foreign N atom. (d) Ground state of O-intercalated system (O_{Bri}), where the atom in red (dark gray) is the foreign O atom.

Bilayer graphene with Bernal stacking was considered in our model. The top view of the bilayer graphene is shown in figure 1(a), in which violet stands for the lower layer, while gray shows the upper layer. As can be seen, position 'Ã' in the lower layer coincides with position 'B' in the upper layer, position 'A' in the upper layer is exactly the center of the hexagon of the lower graphene layer and position 'B̃' in the lower layer is right at the center of the hexagon of the upper graphene layer. The foreign atom is intercalated between the upper and lower graphene layers and is initially set in the middle between them. Three kinds of initial locations were considered for each intercalated atom, i.e. bridge, top and hollow positions, for which the subscripts 'Bri', 'Top' and 'Hol' are used if needed. For example, N_{Bri} is used to indicate the bilayer system with the N atom positioned at the bridge

Table 1. Binding energy (dE), bond length between the adsorption atom and its nearest C atom ($a_{\text{C-atom}}$), and layer spacing of the doped system. The stable position for each intercalated atom is boxed.

	C			N			O		
Position	Top	**Hol**	Bri	Top	Hol	**Bri**	Top	Hol	**Bri**
dE (eV)	1.31	1.93	1.86	0.37	—	1.45	1.68	2.10	2.80
$a_{\text{C-atom}}$ (Å)	1.46	1.54	1.49	1.83	—	1.43	1.74	1.39	1.44
Spacing (Å)	3.53	3.39	3.87	3.62	—	3.87	3.61	3.85	3.76

site. The bridge site is above the carbon–carbon bond in the lower graphene layer, the top site indicates the middle position between the coinciding positions 'Ã' and 'B', and the hollow site is just above one carbon atom of the lower graphene layer and simultaneously below the center of one carbon hexagon of the upper layer. Note that definitions of the top and hollow sites in a Bernal stacking bilayer graphene are somewhat different from those in the monolayer graphene [20].

The binding energy is defined as $dE = E_{\text{graphene}} + E_{\text{atom}} - E_{\text{total}}$, where E_{graphene} is the energy of the clean bilayer graphene, E_{atom} stands for the energy of the single foreign atom and E_{total} is the total energy of the bilayer graphene with the intercalated atom. The binding energy, the length of the bond between the foreign atom and its nearest carbon atom, and the interlayer spacing of the doped bilayer graphene are illustrated in table 1. Ground states with the largest binding energy are boxed in table 1. Both N and O atoms favor the bridge site, while the C atom prefers the hollow site. No intercalated atom is stable at the top site, because the binding energy corresponding to the top site is smallest for each intercalated system. At the top position, the C–N bond length is about 1.83 Å and the C–O bond length is about 1.74 Å, much longer than the typical lengths of C–N (1.47 Å) and C–O (1.42 Å) [21], implying it is physisorption rather than chemisorption. For the hollow site, the O atom is adsorbed to the layer which originally provides the nearest carbon atom, away from the hexagonal center of the other graphene layer, while the length of the C=O bond formed in this system is about 1.39 Å, less than the C–O bond length in O_{Bri} system (1.44 Å). The N_{Hol} structure does not exist because of the negative binding energy obtained. Structure relaxation calculations showed that, if the intercalated atom was initially set at the bridge or hollow site, it would finally be adsorbed into one graphene layer, while for the top site the foreign atom will keep the middle position between the two layers.

Ground states of the intercalated systems, C_{Hol}, N_{Bri} and O_{Bri}, are respectively shown in figures 1(b), (c) and (d). In the C_{Hol} system, the optimized interlayer distance is about 3.39 Å, which is a little larger than the value of 3.34 Å of the pure bilayer graphene. The intercalated C atom pushes down the carbon atom right below it, heavily destroying the structure of the lower graphene layer. Lengths of carbon–carbon bonds between the intercalated C atom and the three adjacent carbon atoms are the same as 1.54 Å, the standard bond length for sp^3 hybridization [21]. In the N_{Bri} system, the layer spacing is enlarged to 3.87 Å and the C–N bond length is 1.43 Å, indicating chemical adsorption rather than physical adsorption. The two carbon atoms bonded with the N atom are drawn away from the graphene layer and the length of the bond between them is 1.55 Å, implying sp^3 hybridization. In the O_{Bri} system, the layer spacing is about 3.76 Å and the C–O bond length is 1.44 Å. The two carbon atoms bonded with the O atom are also drawn away from the graphene layer and the length of the bond between them is 1.51 Å. Obviously, N- and O-intercalated systems have a similar ground state structure, very different from that of the C-intercalated system.

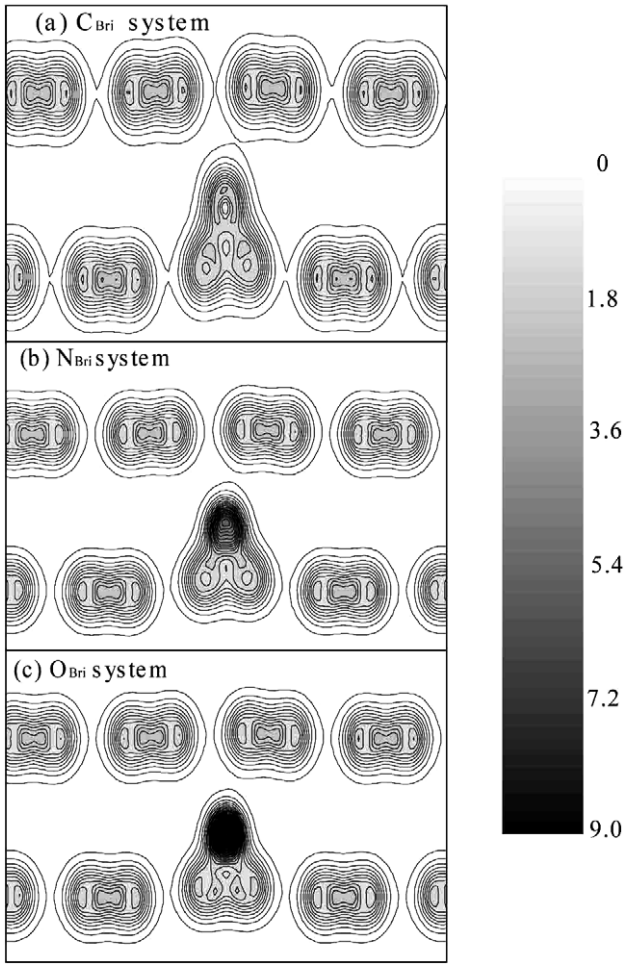

Figure 2. Charge contours of C_{Bri} (a), N_{Bri} (b) and O_{Bri} (c) systems.

3. Results and discussion

The side view of the charge distributions for C_{Bri}, N_{Bri} and O_{Bri} systems is displayed in figure 2. Although the C_{Bri} structure is not the ground state of the C-intercalated system, its charge contour is also shown to provide a clear comparison. We know the O atom is lacking two electrons; when it is adsorbed in the bilayer graphene, it strongly interacts with its adjacent carbon atoms and get electrons from them (see the lower panel of figure 2). The N atom lacks three electrons; it also gets electrons from its adjacent carbon atoms (see the middle panel of figure 2). The C atom lacks four electrons to get saturated, and it tends to share electrons with its adjacent carbon atoms in bilayer graphene (see the upper panel of figure 2). All these three atoms show strong interaction with the lower graphene

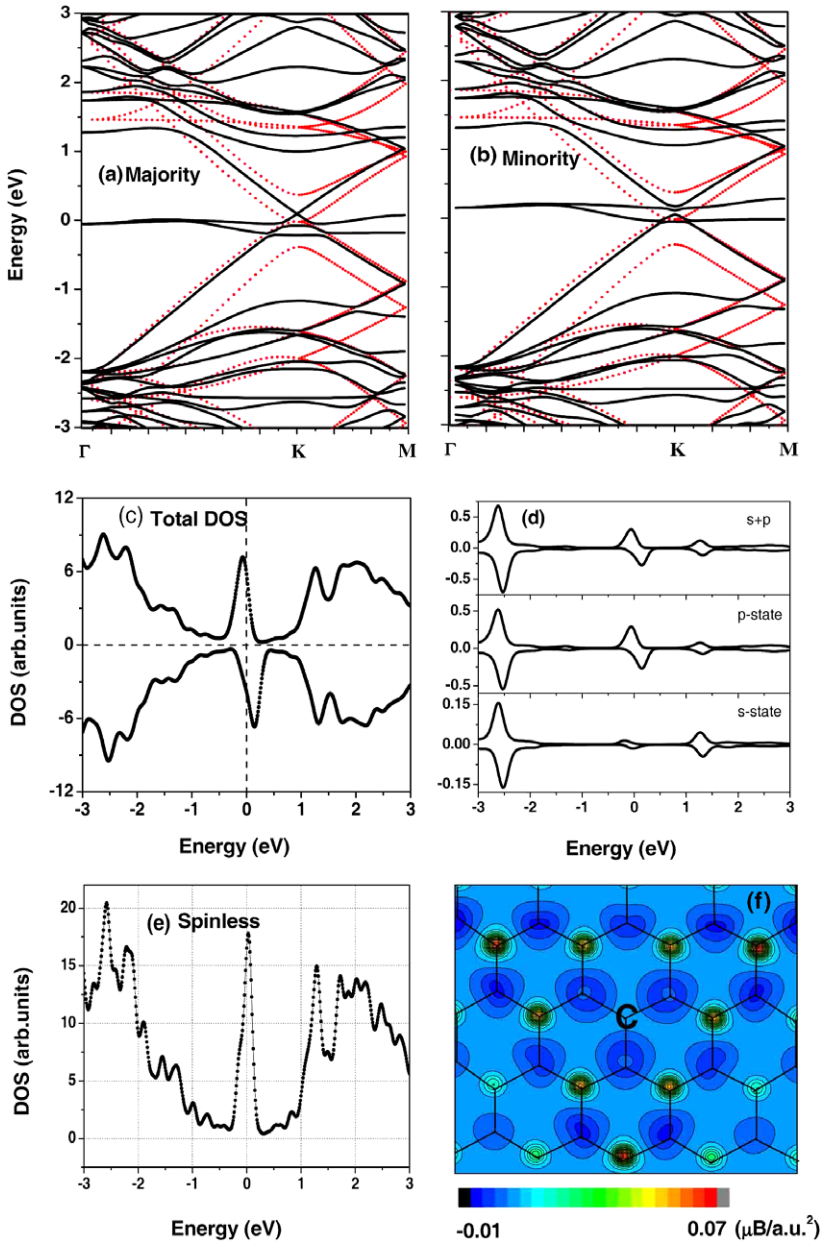

Figure 3. Electronic and magnetic structures of C_{Hol} system. Band structures of the majority spin (a) and minority spin (b), total density of states (c), the orbital-resolved DOS for the foreign C atom (d), density of states for spin unpolarized (spinless) C_{Hol} system (e) and distribution of the spin density on the lower graphene layer (f). The dotted curves in red in (a) and (b) represent band structures of the ideal bilayer graphene. The Fermi level defines the zero of energy, $E_F = 0$.

layer. Concerning their interactions with the upper graphene layer, judging from figure 2, we find the C atom has the strongest interaction with the upper layer, N is the second and O is the third. It is known that, if the interaction between the intercalated atom and the upper graphene layer is weak enough, the stable position of the intercalated atom should be the same as that in monolayer graphene. As we know, N and O atoms adsorbed in monolayer graphene are also stable at the bridge site, the same as that in bilayer graphene, while the C atom is stable at the bridge site in monolayer graphene, but at the hollow site in bilayer graphene. It is believed that the interaction between the intercalated C atom and the upper graphene layer plays the critical role.

The C_{Hol} structure is the ground state of bilayer graphene with an intercalated C atom. Calculated spin-resolved band structures and density of states (DOS) of the C_{Hol} system are shown in figure 3. The Dirac point and the linear energy dispersion, which is characteristic of monolayer graphene, are obtained in the C-intercalated bilayer system. It is believed that they arise from the upper graphene layer, which is less perturbed by the intercalated atom. The π-bond of the lower graphene layer is destroyed by the intercalated atom, resulting in the disappearance of the corresponding π-band. Therefore, the parabolic energy dispersion, which comes from the coupling between the π-bands of upper and lower graphene, are not obtained. Impurity bands for the

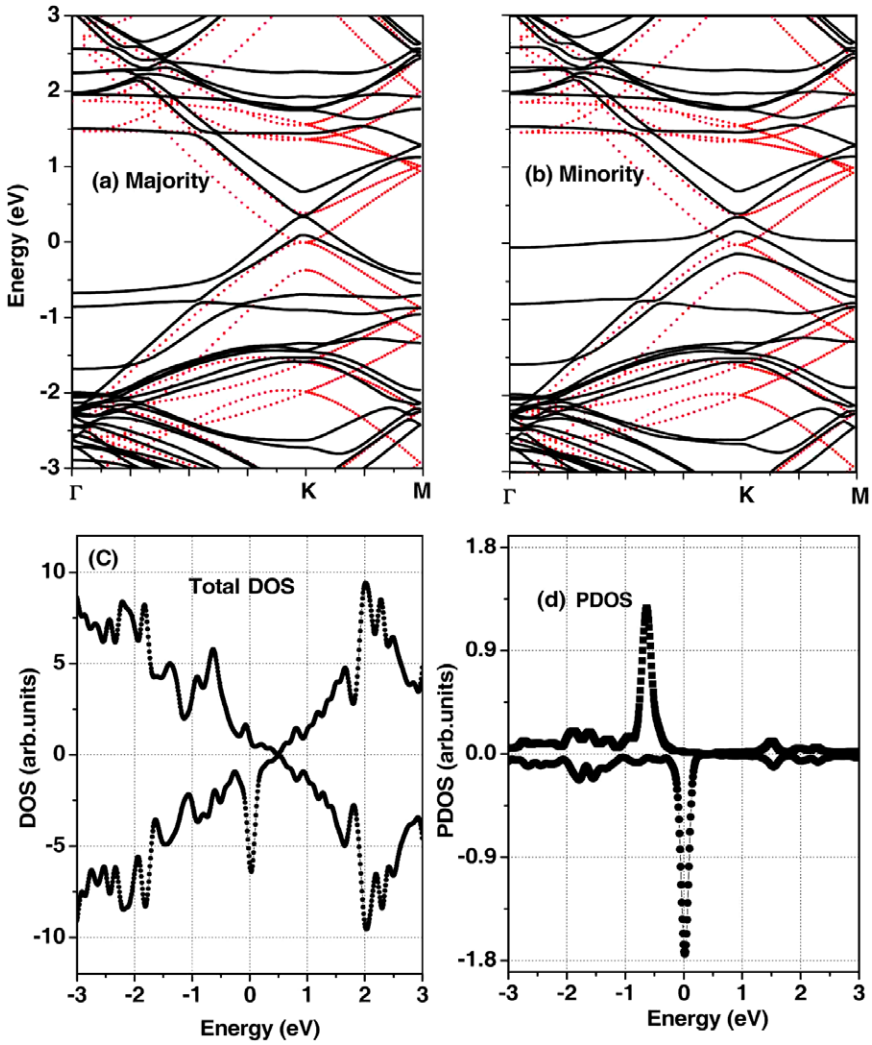

Figure 4. Spin-resolved band structures for majority spin (a) and minority spin (b), total density of states (c) and partial density of states of N atom (d) of N_{Bri} system. The dotted curves in red in (a) and (b) represent band structures of the ideal bilayer graphene.

majority and minority spin components are lower and higher than the Fermi level, respectively. In the majority spin band structure, π states are hybridized with impurity states and the hybridized states have a further effect to electrostatically push the Dirac point shifting upwards to the conduction band, while in the minority spin band structure, an energy gap is opened, with impurity states filled in the gap. Correspondingly, two narrow peaks at the opposite side of the Fermi level are observed in the total DOS plot. The imbalance between the majority and minority spin components around the Fermi level indicates the itinerant magnetism triggered by the intercalated C atom. Partial DOS (PDOS) of the intercalated C atom shows that the foreign C atom is magnetic and its magnetization is mainly contributed by the p-orbital state. In addition, s and p states show peaks in the same energy range, indicating the sp^3 hybridization. The spin density distribution of the lower graphene layer in the C_{Hol} system shown in figure 3(f) indicates that host carbon atoms of the graphene layer also become magnetic, besides the foreign C atom. The magnetic moment distribution of the foreign C atom and the pushed-down carbon atom cannot be seen in figure 3(f), because they are not in the lower graphene plane. Seen from the top view, these two carbon atoms occupy coinciding positions, which are marked in figure 3(f) by the sign 'C'. Clearly, the three nearest carbon atoms bonded with the foreign C atom are nearly nonmagnetic, while the next-nearest neighbors are magnetic. Overall, the spin density distribution on the lower graphene layer shows threefold symmetry, similar to hydrogen adsorption on the graphene plane [22]. Finally, the spin unpolarized (or spinless) calculation is also conducted: a twofold degenerate peak at the Fermi level is obtained, as shown in figure 3(e). But this spin unpolarized state is not the ground state. When the spin degree of freedom is taken into consideration, the very sharp nonmagnetic peak will split into two magnetic peaks and the energy of the system will be decreased.

The bridge site is energetically favored as the stable position for the N atom intercalated in the bilayer graphene. Calculated band structures and density of states of the N_{Bri} system are shown in figure 4. In the majority spin band structure plot, the characteristic conical point at the K-point and parabolic energy dispersion can be clearly identified, implying the bilayer graphene is not strongly perturbed by the

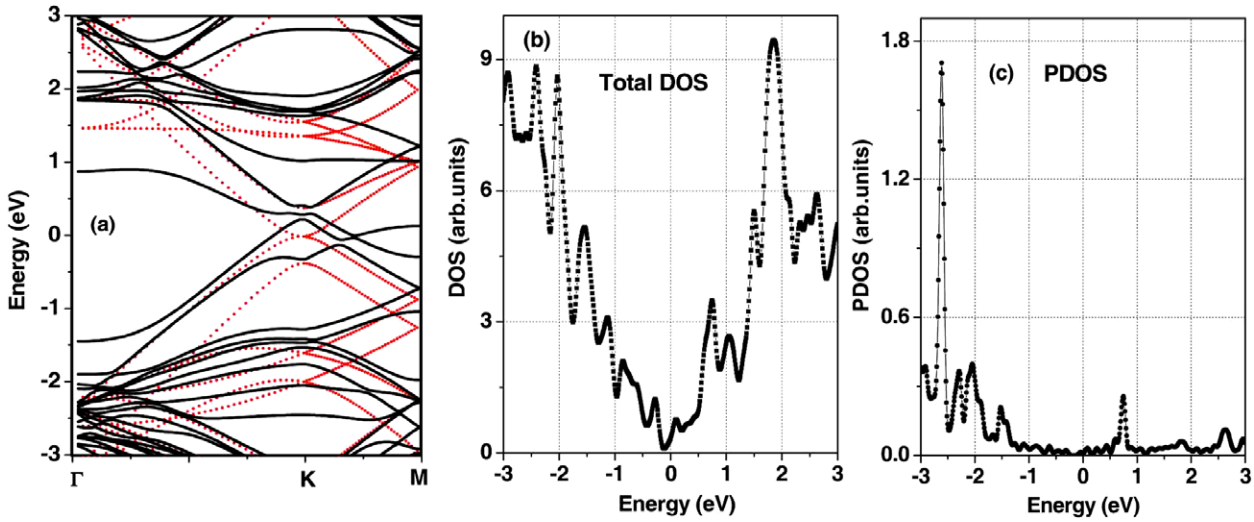

Figure 5. Band structure (a), total density of states (b) and partial density of states of the intercalated O atom (c) of the O_{Bri} system. The dotted curves in red in (a) represent the band structure of the ideal bilayer graphene.

intercalation of the N atom. The critical difference is that, in freestanding bilayer graphene, the Fermi level coincides with the conical point, while the Fermi level in the N-intercalated system is shifted downwards and then below the conical point. A shift downwards (upwards) means the holes (electrons) are provided by the doped atom, for example, manganese doping (electron donor) results in the upward shift of the Fermi level [8]. In the minority spin band structure, an energy gap is opened with the highly localized impurity band filled in the bandgap, similar to the case of the C_{Hol} system. Such a gap is induced by the difference of the electrostatic potential between the two graphene layers introduced by the intercalated atom. A very narrow and sharp peak exists at the Fermi level in the total DOS plot, corresponding to the flat impurity band in the minority spin band structure. Two narrow peaks are obtained in the PDOS of the N atom, one of which is situated at the Fermi level and dominates properties of the N_{Bri} system. This quasilocalized state around the Fermi level gives rise to the strong Stoner magnetism of the N_{Bri} system with a magnetic moment of 0.65 μB. Different from the C-intercalated system, the calculated result shows that magnetization in the N_{Bri} system is only contributed by the N atom, possibly because of the lower hybridization between the doped N atom and the host carbon atoms. Another narrow peak in the PDOS plot is between the energy -0.5 and -1 eV; the corresponding flat impurity band is observed in the majority spin band structure.

The O_{Bri} structure proves to be the ground state of bilayer graphene with an intercalated O atom. Calculated band structure, total density of states and partial density of states of the intercalated O atom are shown in figure 5. Similar to C- and N-intercalated systems, an energy gap filled with impurity states is also obtained in the band structure of the O-intercalated system, as shown in figure 5(a). Calculation results show the O_{Bri} system is nonmagnetic, which is very different from the C- and N-intercalated systems. In both C_{Hol} and N_{Bri} systems, the impurity states localized around the Fermi level introduced by the intercalated atom play the critical role for magnetization. However, such localized states are not obtained in the O-intercalated system; a very low density of states appears around the Fermi level instead, as shown in the PDOS of the intercalated O atom. A peak located around the energy of 0.75 eV is obtained, yet such states cannot bring magnetization for the bilayer graphene. In the band structure plot, a flat impurity band at the energy of 0.75 eV is also observed. In addition, similar to the N_{Bri} system, the O_{Bri} system also undergoes a transition from semi-metal to metallic, with the Fermi level shifting downward to the valence band, which can be seen in figure 5(a).

4. Conclusions

In summary, the structural, electronic and magnetic properties of the bilayer graphene with intercalated C, N or O atoms have been calculated by the *ab initio* density functional theory. Structural relaxation shows that the intercalated atom, initially set at the middle of the layer spacing, will finally be adsorbed into one graphene layer, resulting in the difference of electrostatic potential between the two layers and then an opening of the energy gap filled with impurity states. Both N and O atoms favor the bridge site, while the C atom prefers the hollow site. Intercalation of C or N atoms induces Stoner magnetism by introducing extended or quasilocalized states around the Fermi level. The magnetic moment in the N-intercalated system is mainly contributed by the N atom. In the C-intercalated system, both the foreign intercalated C atom and some host carbon atoms of the graphene layer become magnetic, with the magnetization distribution showing threefold symmetry. In both N- and O-intercalated systems, charge transfer from bilayer graphene to the intercalated atom results in the Fermi level shifting downwards to the valence band and then the metallic behavior of the system.

Acknowledgments

This work was supported by the Ministry of Sciences and Technology through the two 973-Projects (no. 2007CB924901

and no. 2006CB921303), the National Natural Science Foundation of China (grant nos. 60821092 and 1067027).

References

[1] Novoselov K S, Geim A K, Morozov S V, Jiang D, Zhang Y, Dubonos S V, Grigorieva I V and Firsov A A 2004 *Science* **306** 666

[2] Min H, Sahu B, Banerjee S K and MacDonald A H 2007 *Phys. Rev.* B **75** 155115

[3] Zhang Y, Tan Y-W, Stormer H L and Kim P 2005 *Nature* **438** 201

[4] Gusynin V P and Sharapov S G 2005 *Phys. Rev. Lett.* **95** 146801

[5] Wang X, Ouyang Y, Li X, Wang H, Guo J and Dai H 2008 *Phys. Rev. Lett.* **100** 206803

[6] Novoselov K S, Geim A K, Morozov S V, Jiang D, Katsnelson M I, Grigorieva I V, Dubonos S V and Firsov A A 2005 *Nature* **438** 197
Novoselov K S, Jiang D, Schedin F, Booth T J, Khotkevich V V, Morozov S V and Geim A K 2005 *Proc. Natl Acad. Sci. USA* **102** 10451
Geim A K and Novoselov K S 2007 *Nat. Mater.* **6** 183

[7] McCann E and Fal'ko V I 2006 *Phys. Rev. Lett.* **96** 086805
McCann E 2006 *Phys. Rev.* B **74** 161403(R)

[8] Mao Y and Zhong J 2008 *Nanotechnology* **19** 205708

[9] Kuzmenko A B, Heumen E and Marel D 2009 *Phys. Rev.* B **79** 115441

[10] Abergel D S L and Fal'ko V I 2007 *Phys. Rev.* B **75** 155430

[11] Nicol E J and Carbotte J P 2008 *Phys. Rev.* B **77** 155409

[12] Boukhvalov D W and Katsnelson M I 2008 *Phys. Rev.* B **78** 085413

[13] Ohta T, Bostwick A, Seyller T, Horn K and Rotenberg E 2006 *Science* **313** 951

[14] Zhou S Y, Siegel D A, Fedorov A V and Lanzara1 A 2008 *Phys. Rev. Lett.* **101** 086402

[15] Koshino M 2008 *Phys. Rev.* B **78** 155411

[16] Yu E K, Stewart D A and Tiwari S 2008 *Phys. Rev.* B **77** 195406

[17] Lin Y M and Avouris P 2008 *Nano Lett.* **8** 2119

[18] Kresse G and Furthemuller J 1996 *Comput. Mater. Sci.* **6** 15
Kresse G and Furthemuller J 1996 *Phys. Rev.* B **54** 11169
Kresse G and Furthemuller J 1999 *Phys. Rev.* B **59** 1758

[19] Perdew J P, Burke K and Ernzerhof M 1996 *Phys. Rev. Lett.* **77** 3865

[20] Wu M, Liu E Z and Jiang J Z 2008 *Appl. Phys. Lett.* **93** 082504

[21] See http://academic.reed.edu/chemistry/roco/Geometry/bond_distances.html for bond distances

[22] Yazyev O V and Helm L 2007 *Phys. Rev.* B **75** 125408